The Luminescence of Tris(2,2′-bipyridine)ruthenium(II) Dichloride[1]

Fred E. Lytle and David M. Hercules

Contribution from the Department of Chemistry and Laboratory for Nuclear Science, Massachusetts Institute of Technology, Cambridge, Massachusetts 02139.
Received August 9, 1968

Abstract: No previously published explanation of the luminescence of tris(2,2′-bipyridine)ruthenium(II) dichloride has been completely adequate in explaining all of the experimental data. Evidence is presented in this paper that supports assignment of the emission as charge-transfer, spin-forbidden luminescence. Spin–orbit coupling existing in the complex enhances the probability of singlet–triplet transitions and yields an abnormally short-lived phosphorescence. In an EPA solvent, the rate constants for phosphorescence, triplet internal conversion, singlet internal conversion, fluorescence, and intersystem crossing have been determined as $k_p = 2.9 \times 10^5$ sec^{-1}, $k_{ic}^3 = 3.1 \times 10^5$ sec^{-1}, $k_{ic}^1 = 5 \times 10^8$ sec^{-1}, $k_f \sim 4 \times 10^5$ sec^{-1}, and $k_{ix} \geq 5 \times 10^{10}$ sec^{-1}, respectively.

Ruthenium is a group VIII second-row transition element having a [Kr]4d^6 electronic configuration in the dipositive oxidation state. 2,2′-Bipyridine is a well-known chelating agent and is fully discussed in the review by Brandt, *et al.*[2] Of the group VIII elements, cobalt, ruthenium, rhodium, osmium, indium, and platinum have been reported to form luminescent complexes.[3]

The first published account discussing the origin of the luminescence of tris(2,2′-bipyridine)ruthenium(II) dichloride, hereafter referred to as $Ru(bipyr)_3Cl_2$, was by Paris and Brandt.[4] These authors treated the emission as a $\pi^* \rightarrow$ d charge-transfer fluorescence. In his Ph.D. thesis, however, Paris[5] described the process as phosphorescence; Porter and Schläfer[6] referred to the emission as a d* → d phosphorescence, and Crosby, *et al.*,[7] concurred with the d* → d transition type but concluded that the emission was fluorescence. Subsequently, Crosby and Klassen[8] presented new evidence indicating a charge-transfer assignment. They did not suggest the emitting state multiplicity. However, Crosby and Demas[9] did propose phosphorescence on the basis of the long luminescence lifetime at 77 °K.

The purpose of the present investigation is to clarify the reported data and to establish the luminescence mechanism. A charge-transfer spin-forbidden transition adequately explains all of the experimental observations.

Experimental Section

Chemicals. All solvents employed were Matheson Coleman and Bell Spectroquality solvents. The $Ru(bipyr)_3Cl_2$ was purchased from G. Frederick Smith Chemical Co. It was twice recrystallized from distilled water before use.

Solutions. Precautions were necessary for two solvents. In 50% sulfuric acid, the complex is slowly air oxidized to the tripositive state. Thus, all solutions were prepared using previously deoxygenated solvent. In EPA (five parts diethyl ether, five parts isopentane, two parts ethyl alcohol by volume), the complex decomposes over a period of several days to an unidentified product. All measurements with this solvent were made within 24 hr of preparation.

Spectra. All spectral measurements, except those in the ultraviolet, were made using Beckman 1-cm² Pyrex cells modified by the addition of 8-mm Pyrex stems. All solutions were deoxygenated in these cells by bubbling with nitrogen for at least 15 min; then they were frozen solid and a vacuum was applied. The stems were sealed by heating and collapsing the tubing.

Absorption spectra were recorded using a Cary Model 14 spectrophotometer. Emission spectra were recorded with a fluorometer constructed from Aminco building blocks. The photomultiplier was an EMI 9558 QA having an S-20 spectral response. Its temperature was held at −30° using a Products for Research Model TE-104 thermoelectrically cooled chamber. The photomultiplier was powered by a Kepco Model ABC 2500 M dc voltage supply, and the anode current was detected and amplified by a Hewlett-Packard Model 412 A VTVM. The detector output was recorded on a Moseley Model 7005 B X–Y recorder.

The detector–monochromator combination was calibrated utilizing an NBS standard lamp.[10] The source–monochromator combination was calibrated using a Rhodamine-B quantum converter.[11]

Lifetimes. The solutions were excited with a TRW Model 31 A nanosecond spectral source. The emission was detected with an RCA 7265 photomultiplier. The signal, measured across a 50-ohm load resistor, was preamplified with a Tektronix Model 1Al vertical plug-in and was displayed on a Model 556 oscilloscope. The data were recorded with a Tektronix Model C-12 oscilloscope camera and Polaroid Type 107 film.

The pulse width of the source was insignificant in comparison to the decays measured, and simple log intensity *vs.* time plots were used to calculate the lifetimes.

Temperature Control and Measurement. For spectral measurements above ambient, temperature control was achieved with an Instrumentation Laboratory constant-temperature bath, Model 127. Below ambient, an Air Products Cryo-Tip nitrogen refrigerator, Model AC-1-110, was utilized having a Spectroscopy Shroud WMX-1 modified to accommodate the 1-cm² Beckman cells. Gas flow through the refrigerator was controlled with an Air Products Model 0C-11 gas-control panel. This panel was modified by replacing the provided high-pressure shut-off valve with a Whitey micro-regulation valve, Model 22-RS4-A.

---

(1) (a) This work is supported in part through funds provided by the Atomic Energy Commission under Contract No. AT(30-1)-905. (b) Taken from the Ph.D. Thesis of F. E. Lytle, Massachusetts Institute of Technology, 1968. (c) Presented at the 155th National Meeting of the American Chemical Society, San Francisco, Calif., April 1968.

(2) W. W. Brandt, F. P. Dwyer, and E. G. Gyarfas, *Chem. Rev.*, **54**, 959 (1954).

(3) (a) G. A. Crosby, *J. Chim. Phys.*, **64**, 160 (1967); (b) K. R. Wunschel and W. E. Ohnesorge, *J. Amer. Chem. Soc.*, **89**, 2777 (1967); (c) W. E. Ohnesorge in "Fluorescence and Phosphorescence Analysis," D. M. Hercules, Ed., Interscience, New York, N. Y., 1966, Chapter 4.

(4) J. P. Paris and W. W. Brandt, *J. Amer. Chem. Soc.*, **81**, 5001 (1959).

(5) J. P. Paris, Ph.D. Thesis, Purdue University, Lafayette, Ind., 1960.

(6) G. B. Porter and H. L. Schläfer, *Ber. Bunsenges. Physik. Chem.*, **68**, 316 (1964).

(7) G. A. Crosby, W. G. Perkins, and D. M. Klassen, *J. Chem. Phys.*, **43**, 1498 (1965).

(8) D. M. Klassen and G. A. Crosby, *ibid.*, **48**, 1853 (1968).

(9) J. N. Demas and G. A. Crosby, *J. Mol. Spectrosc.*, **26**, 72 (1968).

(10) (a) C. A. Parker and W. T. Rees, *Analyst*, **85**, 587 (1960). (b) The authors are greatly indebted to G. K. Turner for suggestions concerning the experimental aspects of detector calibration.

(11) G. Weber and F. W. J. Teale, *Trans. Faraday Soc.*, **53**, 646 (1957).

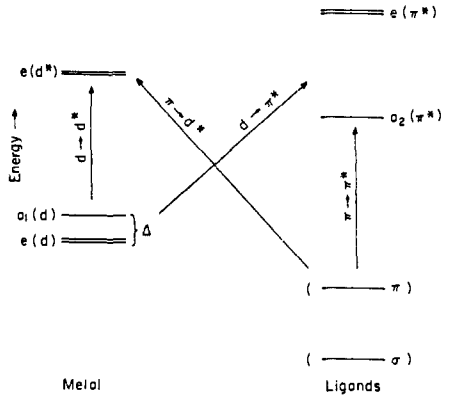

Figure 1. Orbital diagram for $Ru(bipyr)_3Cl_2$ consistent with D_3 symmetry. The metal ion has a $[Kr]4d^6$ low-spin configuration. The ligands have all of the σ and π orbitals filled. Δ is the trigonal splitting.

Above ambient, temperatures were measured with a mercury thermometer. Below ambient, the voltage from a calibrated thermocouple was measured with a Leeds and Northrup Type K-3 universal potentiometer.

Results and Discussion

Transition Types. Figure 1 shows the orbital diagram for $Ru(bipyr)_3Cl_2$, consistent with D_3 symmetry, used in this paper for the classification of transition types. Most discussions of the electronic properties of $Ru(bipyr)_3Cl_2$ have assumed an orbital diagram compatible with octahedral microsymmetry of the ruthenium–nitrogen skeleton, even though the over-all symmetry of the complex is D_3. The only significant difference between the two symmetries is the separation of the $t_{2g}(d)$ orbitals into $a_1(d)$ and $e(d)$ components.[12] The energy separation, Δ, of these components will depend upon the amount of trigonal splitting, which has been determined to be 0.20 μ^{-1} for this complex. As Palmer and Piper have shown,[13] this splitting is not necessarily related to a geometric distortion from the O_h microsymmetry, but may also be due to a degree of covalency in the bonding. Calculations in our laboratory[14] have shown that σ bonding alone can yield the trigonal splitting observed in both this bipyridine complex and those discussed by Palmer and Piper.[13]

The electronic transitions of $Ru(bipyr)_3Cl_2$ can be separated into four general categories as shown in Figure 1. The first are the ligand $\pi \rightarrow \pi^*$ transitions; $\pi \rightarrow a_2(\pi^*)$ and $\pi \rightarrow e(\pi^*)$. The second are the $d \rightarrow d^*$ metal transitions: $e(d) \rightarrow e(d^*)$ and $a_1(d) \rightarrow e(d^*)$. The third are the charge-transfer $d \rightarrow \pi^*$ transitions: $e(d) \rightarrow a_2(\pi^*)$ and $a_1(d) \rightarrow a_2(\pi^*)$, and $e(d) \rightarrow e(\pi^*)$ and $a_1(d) \rightarrow e(\pi^*)$. The fourth is charge-transfer $\pi \rightarrow d^*$ transition: $\pi \rightarrow e(d^*)$. Since the electronic states will be strongly mixed, it is not proper, other than for classification, to treat the ligand and metal orbitals as two separate manifolds.

The two low-energy charge-transfer $d \rightarrow \pi^*$ transitions are both electronically allowed. The $e(d) \rightarrow a_2(\pi^*)$ transition, designated $\perp$CT, is polarized perpendicular to the C_3 axis of the complex, while the $a_1(d) \rightarrow a_2(\pi^*)$ transition, designated $\parallel$CT, is polarized parallel to the C_3 axis. This agrees with the single-crystal absorption data of Palmer and Piper.[13] According to their data the $\parallel$CT band has a low intensity. This is probably due to a lack of overlap of the $a_1(d)$ orbital with the $a_2(\pi)$ orbitals.

(12) In the notation used in this paper, d indicates a metal orbital and π will indicate a ligand orbital.

(13) R. A. Palmer and T. S. Piper, *Inorg. Chem.*, **5**, 864 (1966).

(14) D. Henrie and D. M. Hercules, unpublished studies, MIT, 1968.

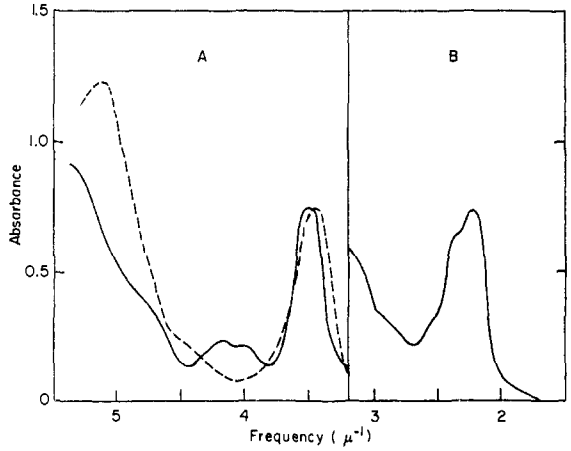

Figure 2. (A) ———, $Ru(bipyr)_3Cl_2$, 1×10^{-4} M in H_2O, 1-cm path length; - - - - -, 2,2′-bipyridine, 2.5×10^{-5} M in 50% H_2SO_4, 1-cm path length. (B) $Ru(bipyr)_3Cl_2$, 5×10^{-4} M in H_2O, 1-cm path length.

Absorption and Emission Spectra

The absorption spectrum of the $Ru(bipyr)_3Cl_2$ complex is shown in Figure 2. No large solvent effects were observed on either the locations of the maxima or the intensity of the absorption bands. To aid in the identification of the $\pi \rightarrow \pi^*$ transitions, Figure 2 also shows the spectrum of the ligand in 50% sulfuric acid. In this medium, both nitrogens are protonated and the electronic properties will be similar to those formed in the coordinated compound. The bonds in the chelate spectrum at 3.50 and 5.40 μ^{-1} can thus be assigned as those derived from the ligand $\pi \rightarrow \pi^*$ transitions, $\pi \rightarrow a_2(\pi^*)$ and $\pi \rightarrow e(\pi^*)$, respectively, according to the nomenclature of Figure 1. The unusual broadness of the ligand $\pi \rightarrow a_2(\pi^*)$ band in comparison to that for the chelate can be attributed to rotation about the 2,2′ carbon bond of bipyridine. This conclusion is substantiated by the protonated ligand band width in an EPA solid matrix; it is identical with that for the chelate in liquid solution.

The two remaining intense bands, at *ca.* 2.3 and 4.1 μ^{-1}, in the chelate spectrum have been assigned as charge-transfer $d \rightarrow \pi^*$ transitions on the basis of Jørgensen's[15] assignments for similar complexes. Both of these charge-transfer bands have two vibronic components resolved at room temperature, 4.20 and 4.00 μ^{-1} for the high-energy transition and 2.37 and 2.20 μ^{-1} for the low-energy transition. There is a reversal in the intensities of the vibronic components of the *ca.* 4.1-μ^{-1} band in comparison to those of the *ca.* 2.3-μ^{-1} band. This difference is probably caused by a $\pi \rightarrow e(d^*)$ charge-transfer transition buried underneath the high-energy transition. The classification of transition types for absorption bands of lower intensity cannot be made with certainty. The shoulder at 4.80 μ^{-1} can be attributed to a $\pi \rightarrow \pi^*$ transition, since it also appears in the ligand spectrum. The bands at 2.90 and 3.10 μ^{-1}

(15) C. K. Jørgensen, *Acta Chem. Scand.*, **11**, 166 (1957).

could be the metal $a_1(d) \rightarrow e(d^*)$ and $e(d) \rightarrow e(d^*)$ transitions.

Low-temperature absorption and emission spectra of the chelate are shown in Figure 3. Both the emission and absorption bands exhibit a regular vibronic progression; the spacing of the absorption band is *ca.* 0.17 μ^{-1} while that of the emission band is *ca.* 0.13 μ^{-1}. Crosby and Klassen[8] attributed these progressions to a perturbed vibration of the aromatic ring. Some doubt concerning this conclusion is found in the paper by Schilt and Taylor,[16] which compares the infrared spectrum of 2,2′-bipyridine with several of its metal chelates. The ring frequencies of the free 2,2′-bipyridine were assigned to bands at 1450 and 1600 cm^{-1}. In all cases it was observed that the ring frequencies were increased upon coordination. Thus it is improbable that the 0.13-μ^{-1} emission progression is due to a perturbed vibration of the aromatic ring.

Schilt and Taylor[16] obliterated a large segment of the spectral region by measuring the infrared spectra of the perchlorate salts of the metal chelates in Nujol mulls. We have recorded the infrared spectra of the 2,2′-bipyridine and the chloride salt of its ruthenium(II) chelate in potassium bromide pellets. A comparison of the two spectra indicates a 1:1 correspondence between most of the ligand and chelate bonds. However, two new bands are conspicuously evident in the chelate spectrum that are not in the ligand spectrum. They are located at 1450 and 1310 cm^{-1}. With the amount of experimental data presently available, it is impossible to determine with certainty the origin of these bands. However, it is possible that both the emission progression and the new infrared bands are due to ruthenium–nitrogen skeletal vibrations from structures such as

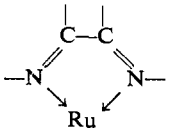

Long-Wavelength Absorption Band. The long-wavelength absorption tail in the vicinity of 1.8–1.9 μ^{-1} cannot be due to the normal tailing of an electronic transition because of the large frequency difference of 0.50 μ^{-1} between the emission and the absorption peaks. Crosby, *et al.*,[7] suggested that this absorption tail was due to a $d \rightarrow d^*$ transition. However, Palmer and Piper[13] demonstrated that the d-orbital split ($10Dq$) would be very large for the $Ru(bipyr)_3Cl_2$ complex, and any $d \rightarrow d^*$ spin-allowed transitions would appear at energies higher than the charge-transfer band at *ca.* 2.3 μ^{-1}.

Crosby and Klassen[8] later assumed that the long-wavelength tail was due to vibronic components of the $\perp$CT band. This assumption leads to unresolvable difficulties. First, it can be demonstrated that the emission observed cannot arise from a spin-allowed transition associated with the $\perp$CT band at *ca.* 2.3 μ^{-1}. Using the equations given by Suzuki[17] for determining intrinsic lifetimes from absorption data, and the integrated band intensity[18] given by Palmer and Piper,[13] a value of 87 nsec can be calculated if the emission came from the excited state associated with the $\perp$CT band. The experimental lifetime at 80°K is about 4 μsec, inconsistent with such an interpretation.

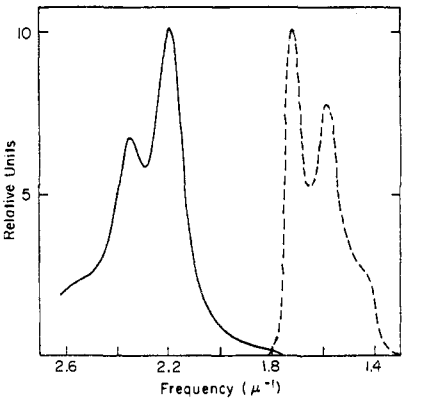

Figure 3. Absorption (——) and emission spectra (- - - -) of $Ru(bipyr)_3Cl_2$ in an ethanol–methanol (5:1) glass at 77°K. The luminescence is corrected for detector–monochromator response.

Second, Crosby and Demas,[9] in assigning the emission as phosphorescence, indicated that there is no gap between the end of the absorption band and the start of the emission. If the singlet–triplet energy split were very small, at room temperature the lifetime of the emission would be equal to that for the spin-allowed transition, because of the thermal equilibrium established between the lowest triplet and the lowest excited singlet states. This is not experimentally observed.

If the long-wavelength absorption tail were due to the $\parallel$CT transition, the emission could then be due to fluorescence from the excited state associated with this transition. The polarization data of Palmer and Piper[13] show that the $\perp$CT transition is 26.5 times more intense than the $\parallel$CT transition. This yields a calculated fluorescence lifetime of 2.3 μsec for emission from the $\parallel$CT state. However, if the emission were fluorescence, the absence of phosphorescence cannot be explained. The extent of spin–orbit coupling in a molecule containing ruthenium should yield a large rate of intersystem crossing, thus significantly populating the lowest triplet level and partially removing the spin-forbiddenness of phosphorescence. This would result in a high population of the lowest triplet level, and both fluorescence and phosphorescence would be expected at 77°K. Such is not observed.

Paris[5] suggested that the absorption tail on the $\perp$CT band was a singlet–triplet transition. Normally this type of transition would be forbidden, but the spin–orbit coupling will partially remove the applicability of the spin selection rules. An increase in the strength of singlet–triplet transitions would also shorten the lifetime of phosphorescence. It will be shown that Paris' interpretation is consistent with all of our experimental data, that the long-wavelength absorption tail is most probably a singlet–triplet transition, and that the emission is the phosphorescence associated with this transition.

Temperature-Dependent Spectral Properties. Both the luminescence quantum yield and lifetime of $Ru(bipyr)_3Cl_2$ are strongly temperature dependent. Figure 4 shows the lifetime as a function of temperature in two different glass-forming solvent mixtures, ethanol–

(16) A. A. Schilt and R. C. Taylor, *J. Inorg. Nucl. Chem.*, 9, 211 (1959).

(17) H. Suzuki, "Electronic Absorption Spectra and Geometry of Organic Molecules," Academic Press Inc., New York, N. Y., 1967, pp 58–59.

(18) Divided by 3, since there are three ligands.

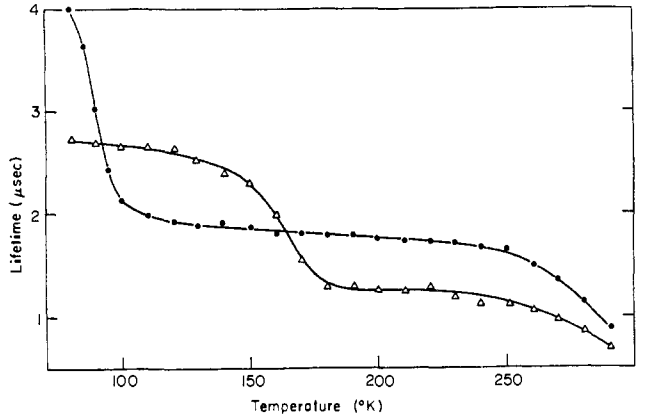

Figure 4. Dependency of the $Ru(bipyr)_3Cl_2$ radiative lifetime on temperature for two glass-forming solvents: (●) ethanol–methanol (5:1), (△) 50% H_2SO_4.

methanol and 50% H_2SO_4. The temperature at which the large increase in lifetime occurs corresponds visually to glass formation. A comparable increase does not occur in the quantum yield, which remains essentially the same before and after glass formation. This indicates that the excited state rate constants important at these temperatures are changed by a multiplicative factor which divides out in the quantum yield expression. Assuming the observed emission is phosphorescence, this multiplicative factor can probably be associated with a decrease in spin–orbit coupling resulting from the rigidity of the glass.

The temperature dependence of the luminescence quantum yield and lifetime, at temperatures above glass formation, is treated mathematically in a manner analogous to that outlined by other workers.[19] The reciprocal of the lifetime can be defined as the sum of all rate constants for reactions depleting the concentration of the excited state responsible for emission. This can be formulated as

$$1/\tau = k_e + \sum_n k'_{dn} + \sum_m k_{dm} \exp(-\Delta H_m/RT) \quad (1)$$

where k_e is the rate constant for the emission process; k_{dn}' is the rate constant for the nth temperature independent nonemissive process; k_{dm} is the frequency factor for the mth temperature dependent nonemissive process; and H_m is the activation energy for the mth temperature-dependent process. The quantum yield can be defined in a similar manner.

If the above mathematical analysis is correct, the value of k_e should be determinable at any temperature by dividing the luminescence quantum yield, ϕ, by the lifetime. The values of τ, ϕ, and k_e are shown in Table I for an EPA solvent. The value of k_e is constant at 2.9×10^5 sec^{-1}, except for 80°K where the solvent glass formation has started.

An assumption of only one important temperature-dependent process can be made at temperatures near ambient. At temperatures from about 200°K and lower to the glass formation point, there seems to be a process occurring that involves a small energy of activation. Again, assuming phosphorescence, this can be tentatively assigned as due to an internal conversion between an excited vibrational level of the lowest triplet state and the ground state. The energy of activation would then be that energy necessary to promote the molecule to the coupled vibrational level of the triplet responsible for this internal conversion process. The data are not sufficiently precise to determine ΔH or k_d.

(19) (a) R. G. Bennett and P. J. McCartin, *J. Chem. Phys.*, **44**, 1969 (1966); (b) E. C. Lim, J. D. Laposa, and J. M. H. Yu, *J. Mol. Spectrosc.*, **19**, 412 (1966).

Table I. Temperature Dependence of the Luminescence Quantum Yield and Lifetime[a]

Temp, °K	ϕ	τ, μsec	k_e, $sec^{-1} \times 10^{-5}$
285	0.270	0.926	2.9
275	0.316	1.07	3.0
265	0.333	1.14	2.9
255	0.360	1.24	2.9
245	0.388	1.36	2.9
235	0.407	1.42	2.9
225	0.418	1.46	2.9
215	0.452	1.53	3.0
205	0.467	1.57	3.0
185	0.515	1.60	3.2
148	0.543	1.87	2.9
103	0.637	2.11	3.0
80	0.746	3.75	2.0

[a] $Ru(bipyr)_2Cl_2$ in EPA, 5×10^{-5} *M*.

If it is assumed that only one temperature-dependent process is operative and if we define $1/\tau' \equiv k_e + \Sigma_n k'_{dn}$, then the Arrhenius equation can be derived from eq 1 as

$$\log(1/\tau - 1/\tau') = -(\Delta H/RT) + k_d \quad (2)$$

An analogous procedure yields the equation

$$\log(1/\phi - 1/\phi') = -(\Delta H/RT) + k_d/k_e \quad (3)$$

where ϕ is the over-all quantum yield of luminescence and $\phi' \equiv k_e/(k_e + \Sigma_n k'_{dn})$.

An Arrhenius plot of the lifetimes using eq 2 yields both the energies of activation and the frequency factors found in Table II. All of the data in this table,

Table II. Arrhenius Constants from Lifetime Data[a]

Constants	H_2O	EPA	DMF	EtOH–MeOH
ΔH, cm^{-1}	885	1400	1600	3100
k_d, sec^{-1}	1.2×10^8	5.0×10^8	2.4×10^4	5.4×10^{12}

[a] For $Ru(bipyr)_3Cl_2$ at 5×10^{-5} *M*.

except that for EPA, were obtained at temperatures above ambient, where the rates of the temperature-independent processes were comparatively small. For EPA, the data were obtained at temperatures below ambient, and the values of the temperature-independent parameters (τ' or ϕ') were empirically established so that the data best fit a linear plot. Figure 5 shows a plot of the corrected data for the EPA solvent.

All mixed solvents employed, except EPA, yielded anomalously large activation energies and frequency factors. In Table II, the ethanol–methanol solvent is shown as a typical example. The cause of the increased Arrhenius constants has not yet been determined.

State Diagram. A state diagram corresponding to a phosphorescence mechanism of luminescence for $Ru(bipyr)_3Cl_2$ is shown schematically in Figure 6. All of the singlet-state energies shown in the diagram were

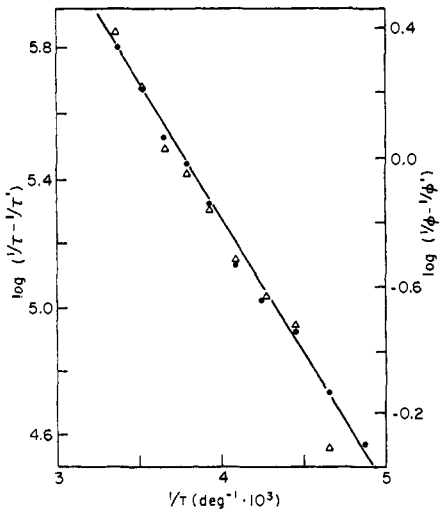

Figure 5. Arrhenius plot of the $Ru(bipyr)_3Cl_2$ luminescence quantum yield and lifetime in an EPA solvent: (Δ) quantum yields with $\phi' = 0.480$; (●) lifetimes with $\tau' = 1.67$ μsec, $\Delta H = 1{,}400$ cm^{-1}; lifetime intercept is 8.70; quantum yield intercept is 3.22.

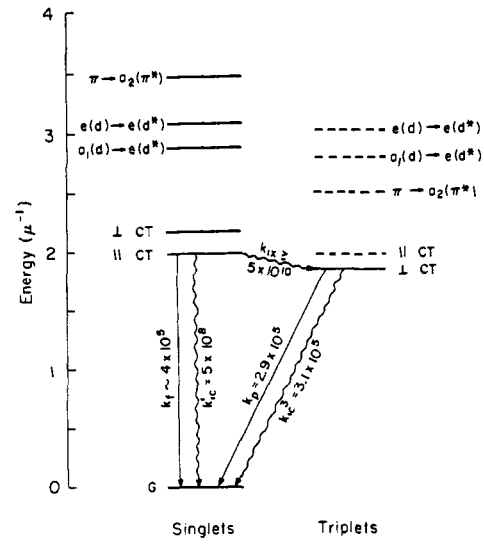

Figure 6. State diagram of $Ru(bipyr)_3Cl_2$: (———) measured energy levels, (- - - -) estimated energy levels. All rate constants are in units of sec^{-1}.

determined directly from absorption spectra except that for the ||CT state. The only triplet-state energy directly determined from absorption and emission spectra was the lowest triplet level.

The transition assignments for the triplet charge-transfer states are consistent with the spectral data. A fluorescence lifetime of 2.3 μsec has been calculated in this paper for the ||CT transition. If the emission were phosphorescence associated with this transition, spin-selection rules would have to be completely removed in order to yield the measured lifetime of 4 μsec. If these selection rules were removed, singlet–triplet absorption bands would occur with the same intensity as singlet–singlet absorption bands. The spectral data do not indicate that this is true; therefore we have assigned the lowest triplet level to the ⊥CT transition.

In pure solvents the Arrhenius data probably represent the deactivation of the lowest excited triplet state by the thermal population of the ||CT band. Since the energy of activation from the Arrhenius plots would represent the lowest triplet to lowest excited singlet energy difference, the energy of the ||CT singlet is thus established.

Using the transition energies shown in Figure 6, the value of $10Dq$ can be calculated to be 2.96 μ^{-1}, while the value of the trigonal splitting can be calculated to be 0.20 μ^{-1}. The magnitude of this trigonal splitting is in agreement with that found by Palmer and Piper[18] for the tris(bipyridine)nickel(II) complex, and the magnitude of $10Dq$ is in agreement with the discussion in their footnote 88.

The intrinsic fluorescence lifetime associated with the ⊥CT transition has been calculated, in this paper, to be 87 nsec. Using the rule that spin-forbidden transitions occur at rates of 10^6 less than those processes spin-allowed, a phosphorescence rate constant (k_p) of 12 sec^{-1} is predicted for the ⊥CT transition. If the emission rate constants (k_c) in Table I were taken to be that of phosphorescence, then the spin–orbit coupling must enhance spin-forbidden processes by a factor of about 10^4. This enhancement would also increase the magnitude of the intersystem crossing rate constant (k_{ix}) to about 10^{11}–10^{12}, since molecules with no large amounts of spin–orbit coupling have corresponding rates of 10^7–10^8.

Two consecutive excited-state processes are involved in the thermal deactivation of the excited triplet. Thus a complex mathematical relationship will be necessary to evaluate the Arrhenius data, unless one of the rate constants associated with these two processes is much larger than the other. Since the frequency factors in Table II are of the magnitude of 10^8–10^9 sec^{-1} and the intersystem crossing rates are expected to be of the magnitude of 10^{11}–10^{12}, the frequency factors can be identified with the singlet internal conversion rate constant (k_{ic}^1), and eq 2 and 3 can be considered valid.

The assignment of the frequency factors as k_{ic}^1 is in agreement with the data in two respects. First, the calculations performed in this paper predict an emission rate constant from the ||CT singlet of 4.3×10^5 sec^{-1}. Since the values of k_{ic}^1 are at least 1000 times larger than the emission rate constant, only 10^{-3} of the thermally populated singlets should emit. To the limit of the instrumentation used, no luminescence to the blue of the phosphorescence could be detected. Second, the quantum yield of phosphorescence should vary with the exciting wavelength to the extent of $k_{ix}/(k_{ix} + k_{ic}^1)$, depending on whether the excitation were on the ⊥CT singlet or the ⊥CT triplet band. With the previously mentioned values of k_{ix} and k_{ic}^1, the ratio should be unity. Experimentally it was determined that k_{ix} must be at least 100 times larger than k_{ic}^1.

The value of the rate constant for internal conversion between the lowest excited triplet and the ground state (k_{ic}^3) can be determined from the measured lifetime and k_p, at any temperature where the thermal population of the excited singlet is negligible. For EPA the lifetime chosen was τ', and the value of k_{ic}^3 determined was 3.1×10^5 sec^{-1}.

Acknowledgment. This work was supported in part through funds provided by the U. S. Atomic Energy Commission under Contract AT(30-1)-905.